

Figure S1.

Figure S1. Generating *flyc1* mutant Venus flytrap plants. Related to Figures 1, 2 and 3.

(A) Diagram of our CRISPR/Cas9 plasmid DNA. Shown is Cas9, kanamycin and hygromycin herbicide resistance cassettes, a 2x35S::*mCitrine* (*mCit*) expression cassette, and gRNAs targeting two sites in each of the *FLYC1* and *FLYC2* genes (g1 through g4).

(B) Image showing selection of regenerated fluorescent transgenic shoot tissue at ~3 months following bombardment. Left, light microscopic image; right, fluorescence microscopic image (green, *mCit*; red, chlorophyll autofluorescence). The total time from bombardment to identification of non-mosaic double mutant plants was 30 months.

(C and D) Schematics of the *FLYC1* (C) and *FLYC2* (D) genes, showing primer locations and the regions PCR amplified for Sanger sequencing-based genotyping. Exons (black boxes), amplified regions (pink boxes), gRNA-targeted sites (blue boxes), and primer binding sites and orientations (black lines and arrows; see STAR Methods) are indicated. The nucleotide positions of the amplified regions are relative to the +1 ATG start sites. The gene structure of *FLYC1* is as previously described^{S1} while *FLYC2* gene structure is generated by aligning the coding sequence of our Venus flytrap strain^{S1} to the previously reported Venus flytrap genome sequence^{S2}.

(E) Genotypes of *flyc1* single mutant lines analyzed in this study. Shown is Sanger sequencing of PCR products from genomic DNA template of wild-type and *flyc1* single mutant lines. The regions shown are overlapping the g1 and g2 CRISPR/Cas9 targeted sites of the *FLYC1* gene, and the g3 and g4 sites of the *FLYC2* gene. Regions are +1058 to +1077 and +1237 to +1256 of the *FLYC1* gene, and +1357 to +1376 and +1516 to +1535 of the *FLYC2* gene. The genotype at each site is indicated (wt indicates wild-type; del indicates deletion). Note that all three single mutant lines are wild type at the g3 and g4 sites of *FLYC2*. The *flyc1* (1069del/1068_1069del) single mutant line was heterozygous for two different mutations at the g1 site: a single base deletion at position +1069 and the deletion of two bases at +1068, creating in-frame stop codons one or 8 codons following the mutation, respectively. This line had additional mutations at the g2 site, displaying heterozygosity for 1247_1250del and 1247_1257del mutations. The other two lines (1069del/1069del lines #1 and #2) showed homozygosity for the single base deletion at position +1069 of the g1 site.

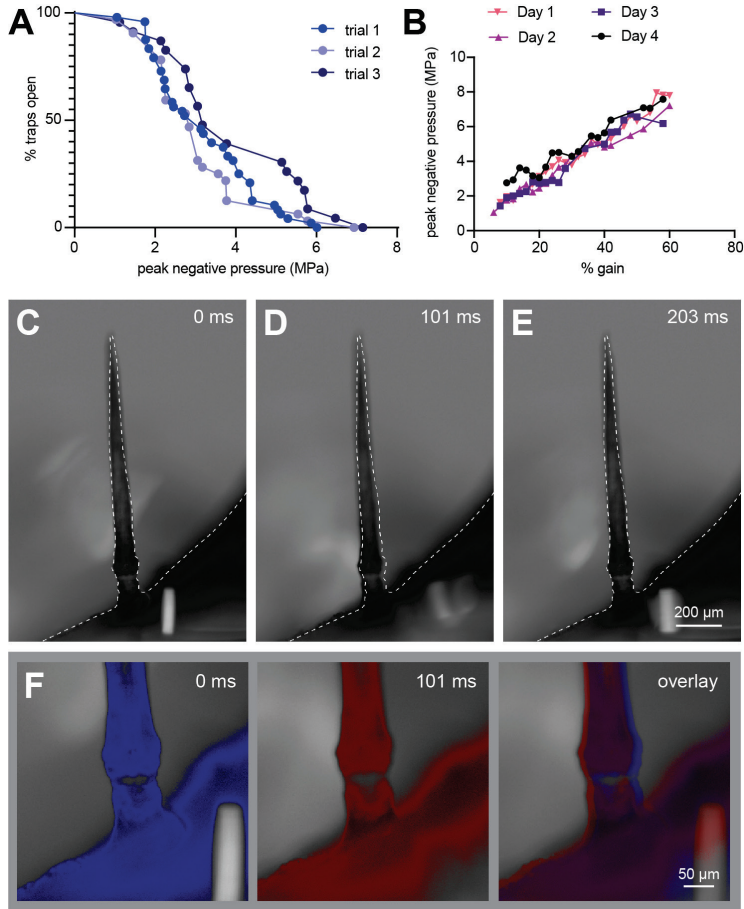


Figure S2. An ultrasound-based assay to measure Venus flytrap leaf closure. Related to Figures 2 and 4.

(A) The peak negative pressure following pulsed ultrasound stimulation required for trap closure of wild-type leaves scored on different days (trials 1-3; $p = 0.067$, logrank test). The days of each trial were > 1 week apart. $n = 48, 32$ and 23 for trials 1 through 3, respectively.

(B) Traps were stimulated by increasing the % gain on a 300-W amplifier attached to an ultrasound transducer and waveform generator (see STAR Methods). The peak negative pressure (PNP) corresponding to the percentage gain on the amplifier was measured over different days, and is similar irrespective of day.

(C-E) Microscopic images showing ultrasound pulsing causing sudden movement of plant tissue. Shown is a dissected piece of Venus flytrap leaf tissue containing a trigger hair mounted on an ultrasound transducer, before (C), immediately following or during (D), and after (E) a 100 ms ultrasound wave pulse (amplifier % gain = 50, corresponding to PNP ≈ 6 MPa). Note the sudden, slight leftward movement of the plant tissue during stimulation in panel D (dashed lines show the initial position of the leaf tissue from panel C). Displacement of the tissue in the x-y plane was 39 ± 11 μm (mean \pm standard deviation; $n = 10$) between frames immediately following ultrasound pulsing.

(F) Close-up view of the base of the trigger hair from panels (C) and (D), false-colored blue and red, respectively (left and middle). Note again the sudden movement of the plant tissue in the overlay image (right). Because the stimulus is extremely rapid (seen in a single microscopic image that fails to capture the complete process of movement), the trigger hair slips in and out of focus, trigger hair movement may be in any orientation in three dimensional space relative to the basal tissue, and presumably any deflection, if present, is extremely small^{S3}, we were unable to assess if an angular deflection of the trigger hair occurs during whole leaf tissue movement.

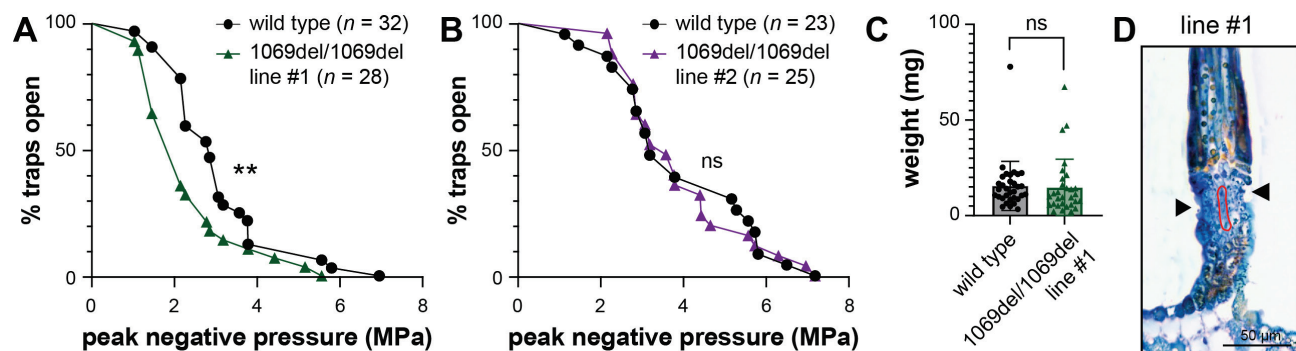


Figure S3. Line-specific effects can be induced by the CRISPR/Cas9-mediated process of mutagenesis. Related to Figures 2 and 4.

(A) The peak negative pressure following pulsed ultrasound stimulation required for trap closure in wild-type and *flyc1* (1069del/1069del) line #1 mutant plants (** $p < 0.005$, logrank test). Wild-type is the same as in Figure 2D (scored simultaneously with *flyc1* mutant 1069del/1068_1069del).

(B) The peak negative pressure following pulsed ultrasound stimulation required for trap closure in wild-type and *flyc1* (1069del/1069del) line #2 mutant plants ($p = 0.825$, logrank test).

(C) Weight of wild-type and *flyc1* (1069del/1069del) line #1 mutant leaf traps scored by ultrasound stimulation in panel (A) (ns, not significant, t-test).

(D) Representative toluidine blue-stained cross-section at the base of the trigger hair of a *flyc1* (1069del/1069del) line #1 mutant plant ($n = 2$). Indentation zone (arrowheads) and an example sensory cell (red outline) are shown.

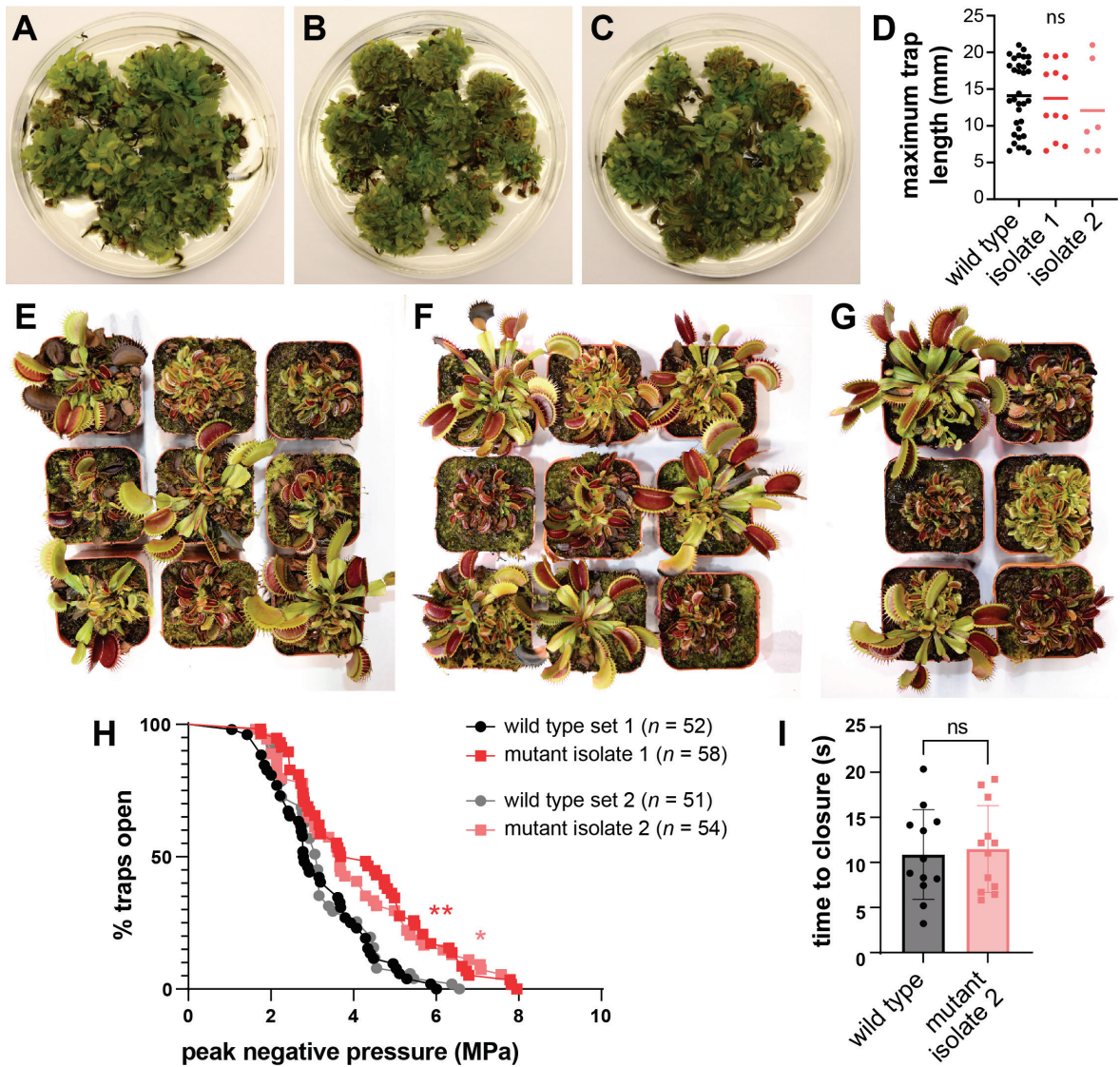


Figure S4. Plants derived from *fylc1 fylc2* double mutant isolates 1 and 2 behave similarly. Related to Figures 3 and 4.

(A-C) Examples of wild-type (A), and *fylc1 fylc2* mutant isolates 1 (B) and 2 (C) growing on 10 cm diameter tissue culture plates.

(D) Maximum trap length (per pot) of wild-type and *fylc1 fylc2* mutant isolates 1 and 2 on soil. Each point represents the average length of the 5 largest leaves for any given pot. ns, not-significant, Kruskal-Wallis test.

(E-G) Examples of wild-type (E), and *fylc1 fylc2* mutant isolates 1 (F) and 2 (G) growing on soil in 5 cm square pots. Note the high variability in trap size between pots, with plants generally displaying either a large-leaf or a small-leaf morphology.

(H) The peak negative pressure following pulsed ultrasound stimulation required for trap closure for wild-type leaves and leaves derived from plants propagated clonally from *fylc1 fylc2* double mutant isolates 1 and 2 (*/** $p < 0.05/0.005$, pairwise logrank tests). The data from the two isolates is combined in Figure 4A.

(I) Time for trap closure in wild-type and *fylc1 fylc2* double mutant (isolate 2) plants. Time reported is immediately following the ultrasound stimulus (at 60% gain), and includes any delay, rapid snapping motion, and slower closing movements until all apparent trap movement has ceased (ns, not significant, t test).

Supplemental References

- S1. Procko, C., Murthy, S., Keenan, W.T., Mousavi, S.A.R., Dabi, T., Coombs, A., Procko, E., Baird, L., Patapoutian, A., and Chory, J. (2021). Stretch-activated ion channels identified in the touch-sensitive structures of carnivorous Droseraceae plants. *eLife* 10. 10.7554/eLife.64250. <https://doi.org/10.7554/eLife.64250>.
- S2. Palfalvi, G., Hackl, T., Terhoeven, N., Shibata, T.F., Nishiyama, T., Ankenbrand, M., Becker, D., Förster, F., Freund, M., Iosip, A., et al. (2020). Genomes of the Venus Flytrap and Close Relatives Unveil the Roots of Plant Carnivory. *Current Biology* 30, 2312-2320.e2315. <https://doi.org/10.1016/j.cub.2020.04.051>.
- S3. Scherzer, S., Federle, W., Al-Rasheid, K.A.S., and Hedrich, R. (2019). Venus flytrap trigger hairs are micronewton mechano-sensors that can detect small insect prey. *Nature Plants* 5, 670-675. <https://doi.org/10.1038/s41477-019-0465-1>.